

Available online at www.sciencedirect.com**ScienceDirect**

Energy Procedia 145 (2018) 64–69

Energy

Procediawww.elsevier.com/locate/procedia

Applied Energy Symposium and Forum, Renewable Energy Integration with Mini/Microgrids,
REM 2017, 18–20 October 2017, Tianjin, China

CFD modeling and simulation of PEM fuel cell using OpenFOAM

Jean-Paul Kone^a, Xinyu Zhang^{a,b,*}, Yuying Yan^{b,c}, Guilin Hu^d, Goodarz Ahmadi^e

^aInternational Doctoral Innovation Centre, University of Nottingham Ningbo China,
199 Taikang East Road, 315100 Ningbo, China

^bResearch Center for Fluids and Thermal Engineering, University of
Nottingham Ningbo China, 199 Taikang East Road; 315100 Ningbo, China

^cFluids & Thermal Engineering Research Group, University of Nottingham,
University Park, NG7 2RD Nottingham, United Kingdom

^dSchool of Mechanical and Automotive Engineering, Zhejiang University of Science and
Technology, No 318, Liuhe Rd, 310023 Hangzhou, China

^eDepartment of Mechanical and Aeronautical Engineering, Clarkson University,
Potsdam, New York, USA

Abstract

A proton exchange membrane (PEM) fuel cell is an electrolytic cell that converts chemical energy of hydrogen reacting with oxygen into electrical energy. To meet increasingly stringent application needs, improved performance and increased efficiency are paramount. Computational fluid dynamics (CFD) is an ideal means for achieving these improvements. In this paper, a comprehensive CFD-based tool that can accurately simulate the major transport phenomena which take place within a PEM fuel cell is presented. The tool is developed using OpenFOAM and it can be used to rapidly gain insights into the cell working processes. The base case results are compared with previous model results and experimental data. The present I-V curve shows better agreement with the experimental trend at low current densities. The simulation data also indicate that the chosen concentration constant has very significant impact on the concentration overpotential.

Copyright © 2018 The Authors. Published by Elsevier Ltd.

Selection and peer-review under responsibility of the scientific committee of the Applied Energy Symposium and Forum, Renewable Energy Integration with Mini/Microgrids, REM 2017

Keywords: Computational fluid dynamics; modelling; numerical; OpenFOAM; proton exchange membrane fuel cell; simulation

* Corresponding author. Tel.: +86-18058261662; fax: +86(0)574 8818 0175.

E-mail addresses: Xinyu.Zhang@nottingham.edu.cn (X. Zhang),

Jean-Paul.KONE@nottingham.edu.cn (J. P. Kone).

1. Introduction

Over the past several decades, fuel cells have become an important low or zero emission energy devices, and thereby an attractive choice for succeeding some of the conventional power devices which depend on fossil fuels. PEM fuel cells have high efficiency and operate at lower temperatures, which make them suitable for automotive power supply, as well as power generation devices for portable electronics and stationary units [1]. The application in the stationary sector covers a wide range of scales going from minigrid-connected combined heat and power systems for residential use, to backup power systems (e.g. uninterruptible power systems (UPS) for buildings, etc.), to main power supply for buildings.

The vast majority of current research work on PEM fuel cells is concern with improving the cell performance by increasing its efficiency meanwhile decreasing the costs associated with manufacturing and test through the CFD technique; and thereby, further promote their rapid integration with mini/microgrid systems. However, until now, truly comprehensive and open-source code PEM fuel cell models are inexistent in the published literature. This work is an attempt to fill this gap.

The model presented in this work is a single-phase flow and non-isothermal model. It is partly an adaptation of the open-source computational model of a solid oxide fuel cell (SOFC) presented by Beale et al. [2] to a PEM fuel cell. This model is different from that of Beale et al. [2] because: it is a different type of fuel cell, the geometry is different, the boundary conditions are different, and the electrochemistry is different.

Nomenclature

c_p	specific heat capacity ($\text{J kg}^{-1} \text{K}^{-1}$)
δ	thickness (m)
F	Faraday's constant ($96485 \text{ C mol}^{-1} \text{ e}^-$)
I	current density (A m^{-2})
k	thermal conductivity ($\text{W m}^{-1} \text{K}^{-1}$)
K	permeability (m^2)
μ	dynamic viscosity (Pa s)
n_i	number of electron of species i
p	pressure (Pa)
ρ	density (kg m^{-3})
ΔS	entropy of formation ($\text{J mol}^{-1} \text{K}^{-1}$)
T	temperature (K)
\vec{U}	velocity (m s^{-1})
y	mass fraction

2. Mathematical Model

2.1. Assumptions

The model assumptions are listed as follows:

- The fuel cell components are isotropic and homogeneous;
- The membrane is assumed to be fully humidified;
- The membrane is impermeable to reactant gases;
- Steady-state operating condition is assumed;
- The gas flow is laminar and incompressible due to low velocities;
- Ideal individual gases and gas mixture are assumed;
- The anode activation and mass transport overpotentials are neglected.

2.2. Governing equations

The conservation equations are expressed by
for mass

$$\nabla \cdot (\rho \vec{U}) = 0 \quad (1)$$

for momentum

$$\nabla \cdot (\rho \vec{U} \vec{U}) = -\nabla p + \nabla \cdot (\mu \nabla \vec{U}) + S_M \quad (2)$$

where S_M is the momentum source term. S_M is equal to zero in the gas flow channels. In the porous media (gas diffusion layers and catalyst layers), S_M is equal to Darcy resistance given by

$$S_M = -\frac{\mu \vec{U}}{K} \quad (3)$$

for chemical species

$$\nabla \cdot (\rho \vec{U} y_i) = (\nabla \cdot \rho D \nabla y_i) \quad (4)$$

where D is the effective diffusivity of species i in $\text{m}^2 \text{s}^{-1}$. The mass fraction of the inert species on each electrode is calculated from the solution of the other species, $y_n = 1 - \sum_{i=1}^{n-1} y_i$

for energy

$$\nabla \cdot (\rho c_p \vec{U} T) = \nabla \cdot (k \nabla T) + S_E \quad (5)$$

where S_E is the energy source term. S_E is essentially due to the heat released by the electrochemical reaction given by

$$S_E = \frac{I}{\delta_{MEA}} \left(\eta - \frac{T \Delta S}{n_i F} \right) \quad (6)$$

The cell voltage is expressed by

$$V_{cell} = E_{Nernst} - \eta \quad (7)$$

where E is Nernst potential and η is the combined voltage loss, also known as overpotential.

2.3. Boundary conditions

Dirichlet boundary conditions are applied at the fluid inlets. The outlet value is prescribed for pressure at the outlets and Neumann boundary conditions are applied at the fluid outlets for all other variables. The membrane-electrode interfaces are insulated against the flow of mass and chemical species. Impermeability, no-slip, and no-flux boundary conditions are applied at all solid-fluid interfaces. A zero-gradient temperature is applied at all the external surfaces of the cell.

3. Numerical Implementation

The present model has been developed using OpenFOAM, a highly flexible open-source CFD software package. Almost every component of the software can be customized to suit the users' needs. Nevertheless, one shortcoming

of the code is that it has no PEM fuel cell module. The pemfcModels-4.0 toolbox developed here is an attempt to provide such a module.

The geometry and mesh of the fuel cell are shown in Fig. 1. A three-dimensional (3D) description of a complete single cell is used. This consists of a membrane electrode assembly (MEA) placed between two bipolar plates (BP). The MEA has two electrodes (i.e. anode and cathode) which are electrically insulated from each other by the membrane. Each electrode has a gas diffusion layer (GDL) and a catalyst layer (CL). For feeding the cell with hydrogen at the anode side and oxygen at the cathode side, gas flow channels (GFC) are cut into the bipolar plates.

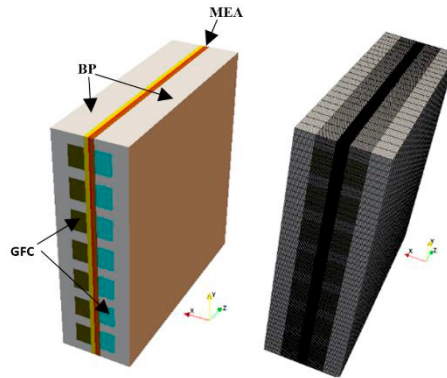


Fig. 1. Geometry and mesh of a single cell PEM fuel cell.

Thus, the modeling domain has multiple regions with multi-physics phenomena existing. This requires different conservation equations to be solved in the different fuel cell components. The solution algorithm follows a specific procedure. After the initialization, several iterations are completed until convergence. For the potentiostatic case the voltage is fixed, whereas for the galvanostatic case the voltage is adjusted until the current density is equal or very close to the initial value. The base case operating conditions are given in Table 1.

Table 1. Base case operating conditions.

Quantity	Symbol	Value	Unit	Source
Cell voltage	V	0.6	V	-
Cell temperature	T_{cell}	353	K	-
Air outlet pressure	p_{air}	101325	Pa	-
Fuel outlet pressure	p_{fuel}	101325	Pa	-
Air inlet velocity	U_{air}	3.082	m s^{-1}	Calculated [3]
Fuel inlet velocity	U_{fuel}	1.1055	m s^{-1}	Calculated [3]
Mass fraction of oxygen	y_{O_2}	0.2	-	-
Mass fraction of water vapor in air	$y_{\text{H}_2\text{O}}$	0.15	-	-
Mass fraction of nitrogen	y_{N_2}	0.65	-	-
Mass fraction of hydrogen	y_{H_2}	0.2	-	-
Fraction of water vapor in fuel	$y_{\text{H}_2\text{O}}$	0.8	-	-
Stoichiometry ratio - cathode air	ξ_{air}	2.0	-	-
stoichiometry ratio - anode fuel	ξ_{fuel}	1.5	-	-

4. Base Case Results

Fig. 2 (a) and 2 (b) show the distribution of hydrogen and oxygen mass fractions, respectively. The mass fractions decrease from the cell inlet to the cell outlet and from the GFCs to the CLs as the electrodes are depleted of the reactants by the electrochemical reaction.

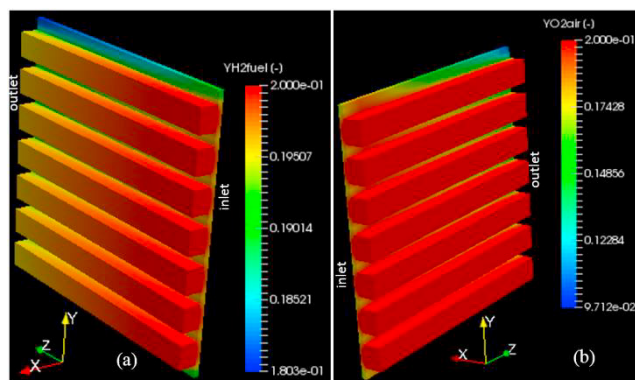


Fig. 2. Species mass fraction distribution (a) Hydrogen; (b) Oxygen.

Fig. 3 (a) illustrates the distribution of the Nernst potential. This decreases from the cell inlet to the cell outlet as the anode is depleted of the fuel due to the combined effects of the consumption of hydrogen and the production of water vapor, which result in a decrease in the observed local current density as shown in Fig. 3 (b). Fig. 3 (c) shows the distribution of the local temperature. Reduced heat sources such as Joule heating and the heat released by the electrochemical reaction under the ribs are the origin of the non-uniform nature of the temperature field. The reduced reaction heat under the ribs is due to lower current densities in these areas due to reduced mass transfer.

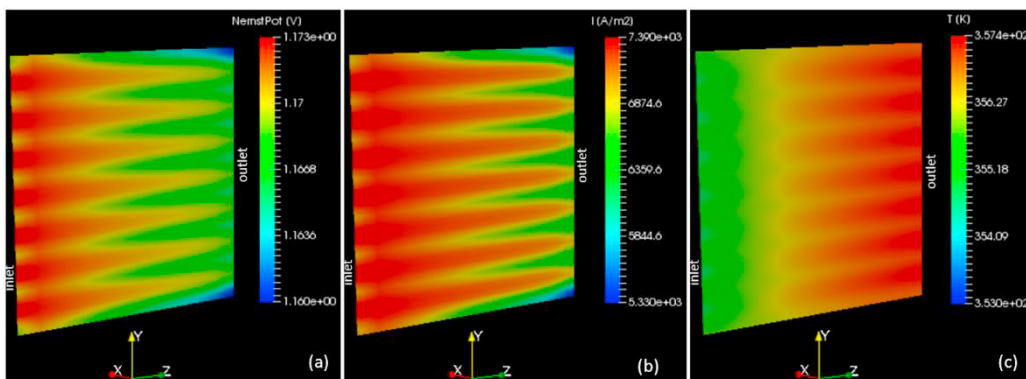


Fig. 3. Membrane cathode interface showing the distribution of (a) Nernst potential; (b) Local current density; (c) Temperature.

Fig. 4 plots the cell polarization or I-V curve. The results of the present work are compared to the results of the numerical model and experimental data reported in Yuan et al. [4] since some of the parameters and properties used in the present model were borrowed from Yuan et al. [4]’s multiphase flow model. The present I-V curve shows better agreement with the experimental trend at low current density, which confirms the validity of the present model. The difference between the present and experimental I-V curves can be attributed to, amongst other things, the combined effects of concentration losses, the cell inlet flow rates, and the consideration of multiphase flow phenomenon. The effective value of the concentration constant is often much larger than its theoretical value, leading to a much larger drop in the current density. Therefore, this constant is often obtained empirically [5]. As for multiphase flow, the

existence of liquid water blocks gas diffusion passages, reduces the diffusion rate and the effective reaction surface area, and hence leads to a deterioration in fuel cell performance.

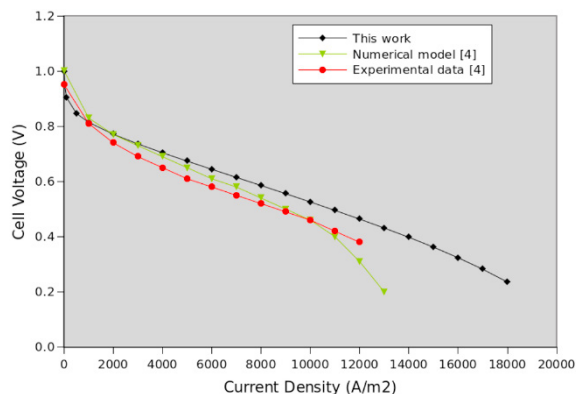


Fig. 4. Polarization curve.

5. Conclusion and Outlook

A toolbox for the numerical simulation of single-phase flow in a PEM fuel cell has been developed using OpenFOAM. The toolbox includes a main program, relevant library classes, and a constructed simulation case for a co-flow galvanostatic simulation.

The base case results are as expected. The plotted polarization curve agrees better with the experimental trend at low current densities compared to a known previous numerical model. Moreover, the simulation data indicate that the value of the concentration constant has significant effects on the cell potential at high current densities.

The provided solver can serve as a basis to develop other features, such as improved catalyst and membrane models, or multiphase flow. Arrangements are being made to make the toolbox available.

Acknowledgements

The authors acknowledge the financial support from the International Doctoral Innovation Centre, Ningbo Education Bureau, Ningbo Science and Technology Bureau, and the University of Nottingham. This work was also supported by the UK Engineering and Physical Sciences Research Council [grant numbers EP/G037345/1 and EP/L016362/1], Faculty of Science and Engineering at University of Nottingham Ningbo China [SRG code 01.03.05.04.2015.02.001], Ningbo Natural Science Foundation Program [project code 2013A610107] and Ningbo Science and Technology Bureau Technology Innovation Team [Grant No. 2016B10010].

References

- [1] Kone JP, Zhang X, Yan Y, Hu G, Ahmadi G. Three-dimensional multiphase flow computational fluid dynamics models for proton exchange membrane fuel cell: A theoretical development. *The Journal of Computational Multiphase Flows*. 2017;9:3-25.
- [2] Beale SB, Choi H-W, Pharoah JG, Roth HK, Jasak H, Jeon DH. Open-source computational model of a solid oxide fuel cell. *Computer Physics Communications*. 2016;200:15-26.
- [3] Liu Z. *Fuel cell performance*. New York: Nova Science Publishers; 2012.
- [4] Yuan W, Tang Y, Pan MQ, Li ZT, Tang B. Model prediction of effects of operating parameters on proton exchange membrane fuel cell performance. *Renewable Energy*. 2010;35:656-66.
- [5] O'Hayre RP, Cha S-W, Colella W, Prinz FB. *Fuel Cell Fundamentals*. New Jersey: John Wiley & Sons; 2006.